Low- and medium-frequency vibroacoustic analysis of complex structures using a statistical computational model and an energy density field formulation.

M. Kassem, Christian Soize, L. Gagliardini

Low- and medium-frequency vibroacoustic analysis of complex structures using a statistical computational model and an energy density field formulation.

M. Kassem[(1),(2)], **C. Soize**[(1)], **L. Gagliardini**[(2)]
(1) Université Paris-Est, Laboratoire de Modélisation et Simulation Multi Echelle, MSME FRE3160 CNRS, 5 Bd Descartes,77454 Marne-la-Vallee, France
(2) PSA Peugeot Citroën, route de Gisy, 78943 Vélizy-Villacoublay, France
e-mail: **morad.kassem@univ-paris-est.fr**

Abstract
In this paper, we present an energy density field approach for low- and medium-frequency vibroacoustic analysis of complex structures using a statistical computational model. The theory presented is adapted to a structure consisting of an automotive vehicle coupled with its internal cavity. The objective of this paper is to take advantage of the statistical properties of the frequency response functions observed from previous experimental and numerical experiences. In this approach, the matrix-valued frequency response function is expressed in terms of a dimensionless matrix which is estimated using the vibroacoustic computational model and the proposed energy method. Using these dimensionless matrix-valued frequency response function a simplified vibroacoustic model is proposed.

1 Introduction

Numerical simulation and mathematical modeling have become more and more complex trying to match numerical models with physical systems. However exact matching is nearly impossible to achieve because of uncertainties existing not only in the parameters of the physical system, but also in the computational model itself. This is why applying statistical methods became necessary to take into account those uncertainties. One well know statistical approach is the parametric probabilistic approach. This approach takes into account uncertainties in the physical system parameters but does not take into account model uncertainties. To take into account model uncertainties the non-parametric probabilistic approach of model uncertainties presented in [1] [2] [3] is used.
In the domain of vibroacoustics, statistical methods are used in the high frequency range where the number of modes is very high and the statistical properties are quite evident. One of the statistical methods used in this frequency range is the Statistical Energy Analysis known as SEA [4][5].This kind of approach and other kinds devoted to the high frequency range have been extensively developed and applied, see for instance developments like [6][7][8][9][10] [11][12][13]. However these approaches are generally not directly applicable to the low- and medium-frequency ranges. In these frequency ranges statistical properties of the response are not evident due to the simultaneous presence of global modes and local modes. Thus, a stochastic approach is necessary for the vibroacoustic analysis of the system to permit taking advantage of the statistical properties of the response in the low- and medium-frequency ranges.
Frequency Response Functions (FRF) between all points of a complex system could be very difficult to analyze specially during a conception phase of an industrial process. Thus a more simplified robust model is needed to simplify these FRF. To achieve such a simplification in the low- and medium-frequency ranges an energy density field approach dealing with these frequency ranges and developed in a statistical context is presented. Note that the proposed approach uses the input and output mobilities to normalize the FRF. this

notion is close to that of the energy mobility introduced in [14] but is a quite different approach.
The stochastic computational model of the vibroacoustic system is obtained from the mean reduced vibroacoustic computational model and using the non-parametric probabilistic approach to take into account both the parameter uncertainties and the model uncertainties. The stochastic equations are then solved using the Monte Carlo method. For shortness, in this paper only the energy analysis and the construction of the simplified model are explained in details. The mean vibroacoustic model is not explained and the reader is referred to [15] for the general formulation and to [16] and [17]for the formulation devoted to automotive structures. The equations of the mean reduced computational vibroacoustic model and those of the stochastic computational model are shown briefly in the first section of this paper. For more details, the reader is referred to [1][2][3][15][16][17].

2 Reduced mean computational vibroacoustic model

The vibroacoustic problem to be solved consists in a three dimensional damped elastic structure without rigid body displacements and is coupled with an internal damped acoustic cavity. For all angular frequency ω belonging to the frequency band of analysis with $B = [\omega_{min}, \omega_{max}]$ with $\omega_{min} > 0$, the reduced mean computational vibroacoustic model is written as

$$\mathbf{u}^s(\omega) = \Psi \mathbf{q}^s(\omega) \quad , \quad \mathbf{p}^f(\omega) = \Phi \mathbf{q}^f(\omega) \quad , \tag{1}$$

in which the $\mathbb{C}^n$-vector $\mathbf{q}^s(\omega)$ of the generalized structural coordinates associated with the n first structural elastic modes constituting the matrix Ψ and the $\mathbb{C}^m$-vector $\mathbf{q}^f(\omega)$ of the generalized acoustical coordinates associated with the m first acoustic modes constituting the matrix Φ which includes the constant pressure mode at zero eigenfrequency, verify the matrix equation

$$\begin{bmatrix} \mathbb{A}^s(\omega) & \mathbb{C} \\ \omega^2\, \mathbb{C}^T & \mathbb{A}^f(\omega) \end{bmatrix} \begin{bmatrix} \mathbf{q}^s(\omega) \\ \mathbf{q}^f(\omega) \end{bmatrix} = \begin{bmatrix} \mathbb{f}^s(\omega) \\ \mathbb{f}^f(\omega) \end{bmatrix} \quad . \tag{2}$$

In Eq. (1), $\mathbf{u}^s(\omega)$ and $\mathbf{p}^f(\omega)$ are the $\mathbb{C}^{n_s}$-vector of the structural DOF and the $\mathbb{C}^{n_f}$-vector of the acoustical DOF. In Eq. (2), $\mathbb{A}^s(\omega)$ and $\mathbb{A}^f(\omega)$ are the generalized dynamical stiffness matrices for the structure and for the acoustic cavity which are written as

$$\mathbb{A}^s(\omega) = -\omega^2 \mathbb{M}^s_n + i\omega \mathbb{D}^s_n + \mathbb{K}^s_n \quad , \tag{3}$$

$$\mathbb{A}^f(\omega) = -\omega^2 \mathbb{M}^f_m + i\omega \mathbb{D}^f_m + \mathbb{K}^f_m \quad . \tag{4}$$

In Eq. (3), $\mathbb{M}^s_n$, $\mathbb{D}^s_n$ and $\mathbb{K}^s_n$ are positive-definite symmetric real $(n \times n)$ matrices corresponding to the generalized mass, damping and stiffness matrices. In Eq. (4) devoted to the acoustic cavity, $\mathbb{M}^f_m$ is a positive-definite symmetric real $(m \times m)$ matrix corresponding to the generalized "mass" matrix and, $\mathbb{D}^f_m$ and $\mathbb{K}^f_m$ are the positive symmetric real $(m \times m)$ matrices corresponding to the generalized "damping" and "stiffness" matrices. Finally, in Eq. (2), $\mathbb{C}$ is the real $(n \times m)$ matrix corresponding to the generalized vibroacoustic coupling matrix and where $\mathbb{f}^s(\omega)$ and $\mathbb{f}^f(\omega)$ are the generalized structural forces and the generalized acoustical sources applied to the vibroacoustic system.

3 Construction of the stochastic reduced computational vibroacoustic model

In this work, the non-parametric probabilistic approach [1][2][3] is used to construct the statistical computational vibroacoustic model in order to take into account both parameter uncertainties and model uncertainties. One refers the reader to [16] for the details of this implementation. In such an approach, the matrices

of the reduced mean computational vibroacoustic model are replaced by random matrices whose mean values are equal, by construction, to the matrices of the reduced mean computational vibroacoustic model. Consequently, Eqs. (1) and (2) are replaced by the following random equations

$$\mathbf{U}^s(\omega) = \Psi \mathbf{Q}^s(\omega) \quad , \quad \mathbf{P}^f(\omega) = \Phi \mathbf{Q}^f(\omega) \quad , \tag{5}$$

in which the $\mathbb{C}^n$-valued random vector $\mathbf{Q}^s(\omega)$ and the $\mathbb{C}^m$-valued random vector $\mathbf{Q}^f(\omega)$ verify the random matrix equation

$$\begin{bmatrix} \mathbf{A}^s(\omega) & \mathbf{C} \\ \omega^2 \mathbf{C}^T & \mathbf{A}^f(\omega) \end{bmatrix} \begin{bmatrix} \mathbf{Q}^s(\omega) \\ \mathbf{Q}^f(\omega) \end{bmatrix} = \begin{bmatrix} \Psi^T \mathbb{f}^s(\omega) \\ \Phi^T \mathbb{f}^f(\omega) \end{bmatrix} \quad , \tag{6}$$

in which the random matrices $\mathbf{A}^s(\omega)$ and $\mathbf{A}^f(\omega)$ are written as

$$\mathbf{A}^s(\omega) = -\omega^2 \mathbf{M}_n^s + i\omega \mathbf{D}_n^s + \mathbf{K}_n^s \quad , \tag{7}$$

$$\mathbf{A}^f(\omega) = -\omega^2 \mathbf{M}_m^f + i\omega \mathbf{D}_m^f + \mathbf{K}_m^f \quad . \tag{8}$$

In Eq. (7), $\mathbf{M}_n^s, \mathbf{D}_n^s$ and $\mathbf{K}_n^s$ are random matrices with values in the set of all the positive-definite symmetric real $(n \times n)$ matrices. In Eq. (8), $\mathbf{M}_n^s$ is a random matrix with values in the set of all the positive-definite symmetric real $(m \times m)$ matrices and, $\mathbf{D}_m^f$ and $\mathbf{K}_m^f$ are random matrices with values in the set of all the positive symmetric real $(m \times m)$ matrices. Finally, in Eq. (6), $\mathbf{C}$ is a random matrix with values in the set of all the real $(n \times m)$ matrices. The probability distributions of these seven random matrices are completely defined in the non-parametric probabilistic approach and a generator of independent realizations of these random matrices is explicitly known(see [1][2][3]). It should be noted that, in this random matrix theory, the statistical fluctuation level of each random matrix is controlled by a dispersion parameter $\delta > 0$. If $\delta = 0$ (deterministic case) the random matrix is equal to its mean value. The larger the value of δ, the larger is the uncertainty level.

4 Explanation of the energy density field approach

Let $\mu = n^s + n^f$ be the total number of DOF. One will only use the subset $\{j_1, \ldots, j_\alpha, \ldots, j_\nu\}$ of the ν observed and excited DOF of the vibroacoustic system. In general, one has $\nu \ll \mu$. Note that the excited DOF are the same as the observed DOF. The excited DOF correspond to external forces applied to the structure and/or to external acoustic sources in the acoustic cavity. For α fixed in $\{1, \ldots, \nu\}$, let $t \mapsto \mathbf{f}^\alpha(t)$ be the function from $\mathbb{R}$ into $\mathbb{R}^\nu$ representing the excitation vector relative to the DOF j_α which is written as $\mathbf{f}^\alpha(t) = \{0, \ldots, f_\alpha^\alpha(t), \ldots, 0\}$ and which is such that $\mathbf{f}^\alpha(-t) = \mathbf{f}^\alpha(t)$. It is assumed that $\mathbf{f}^\alpha$ is square integrable on $\mathbb{R}$. Let $\mathbf{f}^\alpha(\omega) = \int_{\mathbb{R}} e^{-i\omega t} \mathbf{f}^\alpha(t)\, dt$ be its Fourier transform which is real function such that $\mathbf{f}^\alpha(-\omega) = \mathbf{f}^\alpha(\omega)$. Consequently, we have $\mathbf{f}^\alpha(\omega) = \{0, \ldots, f_\alpha^\alpha(\omega), \ldots, 0\}$. finally it will be assumed that the support of $\omega \mapsto \mathbf{f}^\alpha(\omega)$ is the bounded interval $\overline{B} \cup B$ in which $\overline{B} = [-\omega_{max}, -\omega_{min}]$. Let $\mathbb{Z}(\omega)$ be the $(\mu \times \mu)$ complex random matrix such that

$$\mathbb{Z}(\omega) = \begin{bmatrix} \Psi & 0 \\ 0 & \Phi \end{bmatrix} \begin{bmatrix} \mathbf{A}^s(\omega) & \mathbf{C} \\ \omega^2 \mathbf{C}^T & \mathbf{A}^f(\omega) \end{bmatrix}^{-1} \begin{bmatrix} \Psi^T & 0 \\ 0 & \Phi^T \end{bmatrix} \quad , \tag{9}$$

which exists for all ω in B. Let $\mathbf{Z}(\omega)$ be the $(\nu \times \nu)$ complex random matrix such that, for all α and β in $\{1, \ldots, \nu\}$, one has

$$\mathbf{Z}_{\alpha\beta}(\omega) = \mathbb{Z}_{j_\alpha j_\beta} \quad . \tag{10}$$

For all ω fixed in B, let $\mathbf{T}(\omega)$ be the $(\nu \times \nu)$ complex random matrix defined by

$$\mathbf{T}(\omega) = i\omega \mathbf{Z}(\omega) \quad . \tag{11}$$

The function $\omega \mapsto \mathbf{T}(\omega)$ is called the matrix-valued random FRF related to the excited and the observed DOF. It should be noted that $\mathbf{T}(-\omega) = \overline{\mathbf{T}}(\omega)$. Let $\mathbf{V}^{\alpha}(\omega)$ be the ν complex random vector of the velocity responses for the observed DOF $\{j_1, \ldots, j_\nu\}$. One then has

$$\mathbf{V}^{\alpha}(\omega) = \mathbf{T}(\omega)\mathbf{f}^{\alpha}(\omega) \quad . \tag{12}$$

We now introduce the $(\nu \times \nu)$ random mobility matrix $\mathbf{Y}(\omega)$ of the vibroacoustic system for the excited and the observed DOF. Below one uses the terminology introduced in references [18] [19] concerning the driving point mobility functions and the coupling mobility functions. Since we are only interested in the driving point mobility functions and not by the coupling mobility functions, the random mobility matrix is a $(\nu \times \nu)$ real diagonal random matrix defined by

$$\mathbf{Y}_{\alpha\beta}(\omega) = \begin{cases} Re(\mathbf{T}_{\alpha\alpha}(\omega)) & \text{if } \alpha = \beta \\ 0 & \text{if } \alpha \neq \beta \end{cases} \quad . \tag{13}$$

It should be noted that, for all $\omega \in B$, $\mathbf{Y}_{\alpha\alpha}(\omega)$ is positive-valued random variable which is such that $\mathbf{Y}_{\alpha\alpha}(-\omega) = \mathbf{Y}_{\alpha\alpha}(\omega)$.
One now introduces the vector-valued spectral density function $\mathbf{s}^f = (s_1^f(\omega), \ldots, s_\nu^f(\omega))$ belonging to $(\mathbb{R}^+)^\nu$ relative to all the excited DOF such that

$$s_\alpha^f(\omega) = (1/2\pi) f_\alpha^\alpha(\omega)^2 \quad . \tag{14}$$

The random input power of the vibroacoustic system induced by the excitation $\mathbf{f}^{\alpha}$ is defined by

$$\mathbf{\Pi}_{in}^{\alpha} = \int_{\mathbb{R}} \mathbf{f}^{\alpha}(t)^T \, \mathbf{V}^{\alpha}(t) \, dt \quad . \tag{15}$$

which can be rewritten in the form

$$\mathbf{\Pi}_{in}^{\alpha} = \int_B \pi_{in}^{\alpha}(\omega) \, d\omega \quad , \tag{16}$$

where $\pi_{in}^{\alpha}(\omega)$ can be defined by

$$\boldsymbol{\pi}_{in} = (\pi_{in}^1, \ldots, \pi_{in}^{\alpha}, \ldots, \pi_{in}^{\nu}) \tag{17}$$

and it can be demonstrated using the above equations that

$$\boldsymbol{\pi}_{in}(\omega) = 2\mathbf{Y}(\omega)\mathbf{s}^f(\omega) \quad . \tag{18}$$

From Eq. (18), it can be deduced that

$$\mathbf{s}^f(\omega) = \frac{1}{2}\mathbf{Y}(\omega)^{-1}\boldsymbol{\pi}_{in}(\omega). \tag{19}$$

Similarly, One then introduces the $(\mathbb{R}^+)^\nu$-valued random spectral density function $\mathbf{s}^v$ of the velocity responses $\mathbf{V}^1, \ldots, \mathbf{V}^\nu$ such that

$$\mathbf{s}^v(\omega) = (s_1^v(\omega), \ldots, s_\nu^v(\omega)) \quad . \tag{20}$$

where $s_\alpha^v(\omega) = \frac{1}{\pi} \parallel \mathbf{V}^{\alpha}(\omega)$ is The spectral density function of the response velocity $\mathbf{V}^{\alpha}$. Introducing the $(\nu \times \nu)$ real random matrix $\mathbf{H}_{\beta\alpha}(\omega) = |\mathbf{T}_{\beta\alpha}(\omega)|^2$ one can easily deduce that

$$\mathbf{s}^v(\omega) = 2\,\mathbf{H}(\omega)\,\mathbf{s}^f(\omega) \quad . \tag{21}$$

Defining the $(\mathbb{R}^+)^\nu$-valued random local input power density function π_{in}^L such that

$$\mathbf{s}^v(\omega) = \mathbf{Y}(\omega)\boldsymbol{\pi}_{in}^L(\omega) \quad , \tag{22}$$

after simple mathematical calculation one can get

$$\boldsymbol{\pi}_{in}^L(\omega) = \mathbf{Y}(\omega)^{-1}\mathbf{H}(\omega)\mathbf{Y}(\omega)^{-1}\boldsymbol{\pi}_{in}(\omega) \quad . \tag{23}$$

Introducing the $\nu \times \nu$ real full random matrix $\mathcal{E}(\omega)$ defined by

$$\mathcal{E}(\omega) = \mathbf{Y}(\omega)^{-1}\mathbf{H}(\omega)\mathbf{Y}(\omega)^{-1} \quad , \tag{24}$$

it can easily be seen that Eq. (23) can be rewritten as

$$\boldsymbol{\pi}_{in}^{L}(\omega) = \mathcal{E}(\omega)\,\boldsymbol{\pi}_{in}(\omega) \quad . \tag{25}$$

The two fundamental Eqs. (22) and (25) allows $\mathbf{s}^v(\omega)$ to be calculated as a function of $\boldsymbol{\pi}_{in}(\omega)$ via $\boldsymbol{\pi}_{in}^{loc}(\omega)$. Consequently, the random matrix $\mathcal{E}(\omega)$ can be viewed as a random dimensionless operator allowing the random local input power density function to be calculated as a function of the random input power density function. On the other hand, it can be deduced the following fundamental equation

$$\mathbf{s}^v(\omega) = 2\,\mathbf{Y}(\omega)\mathcal{E}(\omega)\mathbf{Y}(\omega)\,\mathbf{s}^f(\omega) \quad . \tag{26}$$

5 Introduction of the local coordinate system

It should be noted that the random equations defined by Eqs. (5) and (6) are relative to the global coordinate system. In this section, one represents the local FRF in a local coordinate system defined by the principal directions of the local mobility. Such a representation allows the type of dominant deformations to be analyzed with respect to the geometry. For instance, at a local point located in a thin shell of the structure, if the most important principal direction is perpendicular to the tangent plane of the shell, then the largest part of the energy of the response will mainly be associated with flexural deformations while if the most important principal direction belongs to the tangent plane, then the largest part of the energy will mainly be associated with membrane deformations.

5.1 Representation of the stochastic system in the new coordinates system

Let $\mathbf{T}_p(\omega)$ be the random matrix with values in the set of all the symmetric complex (3×3) matrices and corresponding to the translational DOF of the random FRF at a given point p of the structure (note that the rotational DOF are not considered here). One then introduces the mean value $E\{\mathbf{T}_p(\omega)\}$ of the random matrix $\mathbf{T}_p(\omega)$ in which E denotes the mathematical expectation. Let $\mathbb{T}_p(\omega)$ be the symmetric real (3×3) matrix such that $\mathbb{T}_p(\omega) = \Re\mathrm{e}\{E\{\mathbf{T}_p(\omega)\}\}$. The representation of the random matrix $\mathbf{T}_p(\omega)$ in the local coordinates attached to the given point and defined by the principal direction of the mean local mobility, is the random matrix denoted by $\mathbf{T}_p^{loc}(\omega)$ and is written as

$$\mathbf{T}_p^{loc}(\omega) = \mathbb{X}_p(\omega)^T\mathbf{T}_p(\omega)\mathbb{X}_p(\omega) \quad . \tag{27}$$

One can now consider the Eq. (24) in the local coordinates for all the local DOF of the structure at points p and all the the global DOF of the acoustic cavity all together which can then be rewritten

$$\mathcal{E}^{loc}(\omega) = \mathbf{Y}^{loc}(\omega)^{-1}\,\mathbf{H}^{loc}(\omega)\,\mathbf{Y}^{loc}(\omega)^{-1} \quad . \tag{28}$$

All other equations of section 4 still hold true in the local coordinates. Thus, these equations are going to be used in what follows with a subscript or a superscript loc to refer to values in these coordinates.

6 Construction of the simplified model

The mean matrix-valued FRF is calculated using the mean value of the Monte Carlo realizations of the FRF after projection on principal directions of the mean local mobility. One can then write

$$\underline{\mathbf{T}}^{loc}(\omega) = E\{\mathbf{T}^{loc}(\omega)\} \quad , \tag{29}$$

and

$$\underline{\mathcal{E}}^{loc}(\omega) = E\{\mathcal{E}^{loc}(\omega)\} \quad . \tag{30}$$

in this case the local mobility is written as

$$\underline{\mathbf{Y}}^{loc}_{\alpha\beta}(\omega) = \begin{cases} Re(\underline{\mathbf{T}}^{loc}_{\alpha\alpha}(\omega)) & \text{if } \alpha = \beta \\ 0 & \text{if } \alpha \neq \beta \end{cases} \quad . \tag{31}$$

Taking the mathematical expectation of Eq. (26) in the local coordinates leads us to

$$E\{\mathbf{s}^v_{loc}(\omega)\} = 2\, E\{\mathbf{Y}^{loc}(\omega)\mathcal{E}^{loc}(\omega)\mathbf{Y}^{loc}(\omega)\mathbf{s}^f_{loc}(\omega)\} \quad . \tag{32}$$

if the the following approximations are introduced then

$$E\{\mathbf{s}^v(\omega)\} = E\{\mathbf{Y}(\omega)\}E\{\boldsymbol{\pi}^L_{in}(\omega)\} \tag{33}$$

$$E\{\boldsymbol{\pi}^L_{in}(\omega)\} = E\{\mathcal{E}(\omega)\}E\{\boldsymbol{\pi}_{in}(\omega)\} \quad , \tag{34}$$

then the approximation $\underline{\mathbf{s}}^v_{loc}(\omega)$ of the $E\{\mathbf{s}^v_{loc}(\omega)\}$ is written as

$$\underline{\mathbf{s}}^v_{loc}(\omega) = 2\underline{\mathbf{Y}}^{loc}(\omega)\underline{\mathcal{E}}^{loc}(\omega)\underline{\mathbf{Y}}^{loc}(\omega)\mathbf{s}^f_{loc}(\omega) \quad . \tag{35}$$

These approximations are shown to be numerically verified in Section 7, taking into account the following construction.
Now, let J and O be the set of excitation and observation DOF respectively such that $J = \{k_q, q = 1, ..., \mu\}$ and $O = \{j_p, p = 1, ..., \nu\}$, where μ and ν are the number of excitation and number of observation DOF respectively as illustrated in Fig.(1).

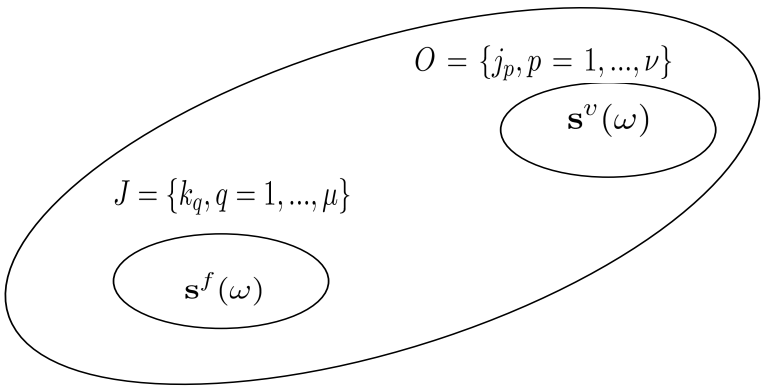

FIG. 1 – Schematic presentation of the sets of excitation and observation points.

Introducing $\mathbb{S}^f_{loc}(\omega)$ as the matrix-valued spectral density function of the excitation forces defined by

$$(\mathbb{S}^f_{loc}(\omega))_{j_p k_q} = \begin{cases} (\mathbf{s}^f_{loc}(\omega))_{j_p} & \text{if } j_p = k_q \\ 0 & \text{if } j_p \neq k_q \end{cases} \quad , \tag{36}$$

and assuming that the excitation and observation DOF J and O are sufficiently distant from each, let e_{OJ} be the real number such that for each ω in the frequency band B, it is assumed that

$$(\underline{\mathcal{E}}^{loc}(\omega))_{j_p k_q} \simeq e_{OJ}(\omega) \quad . \tag{37}$$

In order that this last ussumption be verified, the quantity $e_{OJ}(\omega)$ is computed by the equation

$$e_{OJ} = \frac{\sum_{p=1}^{\nu}(E\{\mathbf{s}^v_{loc}(\omega)\})_{j_p}}{E\{\pi^{loc}_{in}\}\sum_{p=1}^{\nu}(\underline{\mathbf{Y}}^{loc}(\omega))_{j_p j_p}} \quad , \tag{38}$$

where $(E\mathbf{s}^v_{loc}(\omega))_{j_p}$ is the summation over the excitation DOF of the mean random spectral density function of the velocity responses calculated using Eq. (32) and $\underline{\pi}^{loc}_{in}$ is the the summation over the excitation DOF of the mean value of the local input power density function. The value of the approximated mean vector-valued spectral density function of the output velocity can then be recalculated using the matrix $\mathbb{E}_{OJ}$ defined by $(\mathbb{E}_{OJ})_{j_pk_q}(\omega) = e_{OJ}(\omega)$ to obtain the approximated value

$$(\underline{\mathbf{s}}^v_{loc}(\omega))^{app}_{j_p} = e_{OJ}(\omega)\,[\underline{\mathbf{Y}}^{loc}(\omega)]_{jpjp}\,E\{\pi^{loc}_{in}\} \quad . \tag{39}$$

The associated error due to this hypothesis can then be evaluated by defining the matrix $\epsilon^2_{\mathcal{E}}$ of the errors for fixed J and O

$$[\epsilon_{\mathcal{E}}]^2_{j_pk_q} = |[\underline{\mathcal{E}}^{loc}(\omega)]_{jpkq} - [\mathbb{E}_{OJ}(\omega)]_{jpkq}|^2 \quad . \tag{40}$$

7 Application

The application of the proposed method was performed on an automotive vehicle model. the mean model consists of a non-trimmed vehicle structure and it's internal cavity. The coupling between the acoustic fluid and the structure is done using a sub-mesh of the structure which is compatible with the mesh of the internal cavity having 8397 DOF as shown in Fig. (2-b). The structure mesh have 1 042 851 DOF and the internal cavity have 9157 DOF as shown in Fig. (2-a). As mentioned earlier, only translational displacements of the structure are taken into account. Unit excitations forces were placed at each observation DOF on the structure, while unit acoustic sources were placed at each observation DOF in the acoustic cavity. So the number of observation and excitation DOF are equal. Twelve excitation and observation points were chosen in different zones of the internal acoustic cavity, and 28 on the structure with a total of 96 DOF. The points on the structure were mainly chosen to model loads induced by the engine and the front suspension. Other points were placed on the floor board, wind shield, roof, trunk board. The analysis is done in the low-frequency band $B = [50, 350]Hz$.

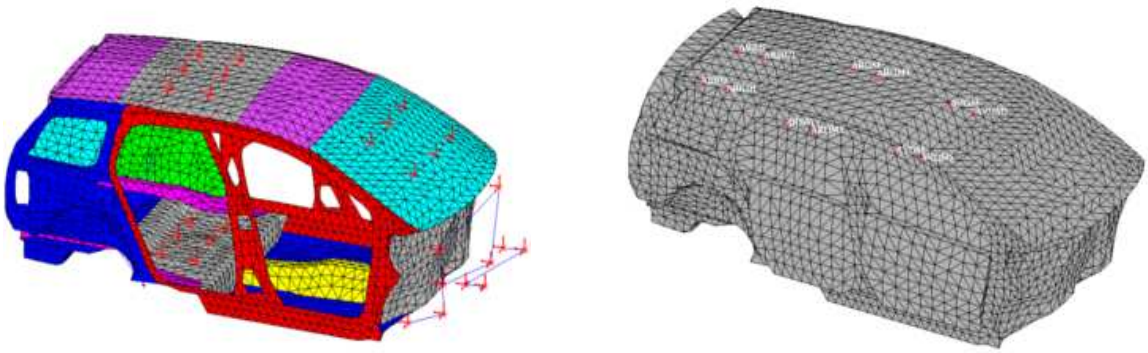

a) Sub-mesh of the finite element model of the structure b) Finite element model of the internal cavity

FIG. 2 – Finite element mesh of the mean model

The modal analysis of the system is performed using Nastran with the system damping rate of 0.04 for the structure and 0.1 for the fluid. The structure has 1955 elastic modes and 3 rigid body translational modes, while the fluid has 160 modes including the zero pressure mode. After obtaining the matrices of the deterministic model from Nastran, the random matrices of the vibroacoustic system are constructed as explained in [1][2][3]. Uncertainties on the mass, damping, stiffness and coupling matrices were considered. The value of the dispersion parameters were selected from previous work on a similar model [17]. The random vibroacoustic equation of the system is then solved using the Monte Carlo solver with n^r Independent realizations.

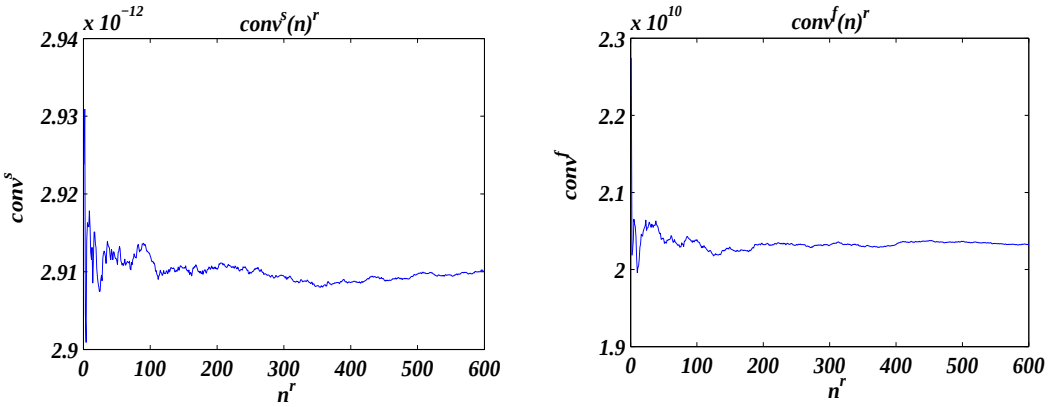

FIG. 3 – Left : convergence function $conv^s(n^r)$ of the structure as a function of the number n^r of realizations. Right : convergence function $conv^f(n^r)$ of the fluid as a function of the number n^r of realizations.

The convergence of the random solution is tested as a function of the number of realizations using the conversion index [2][3] defined by the equation

$$conv^H(n^r) = \frac{1}{n^r} \sum_{\ell=1}^{n^r} \int_B \|\mathbf{Q}^{\mathbf{H}}(w;\theta_\ell)\|^2 d\omega \quad , \tag{41}$$

in which H stands for either the structure s or the fluid f, and $\mathbf{Q}^{\mathbf{H}}(w;\theta_1), ..., \mathbf{Q}^{\mathbf{H}}(w;\theta_{n^r})$ are the independent realization of the vector-valued random variable $\mathbf{Q}^{\mathbf{H}}(w)$. For precision reasons no modal truncation was used and all modes were taken into consideration. The number of modes needed for convergence obtained in previous work on a similar model in [17] shows that the number of modes considered here are sufficient for convergence. Fig. (3) shows the graphs of the convergence functions $conv^s(n^r)$ and $conv^f(n^r)$ of the structure and of the fluid respectively as a function of the number n^r of realizations. Fig. (3) shows that convergence for the structure occurs at about 550 realizations while for the fluid it occurs at about 400 realizations. Thus 600 realizations are chosen to insure convergence of both the structure and the fluid part.

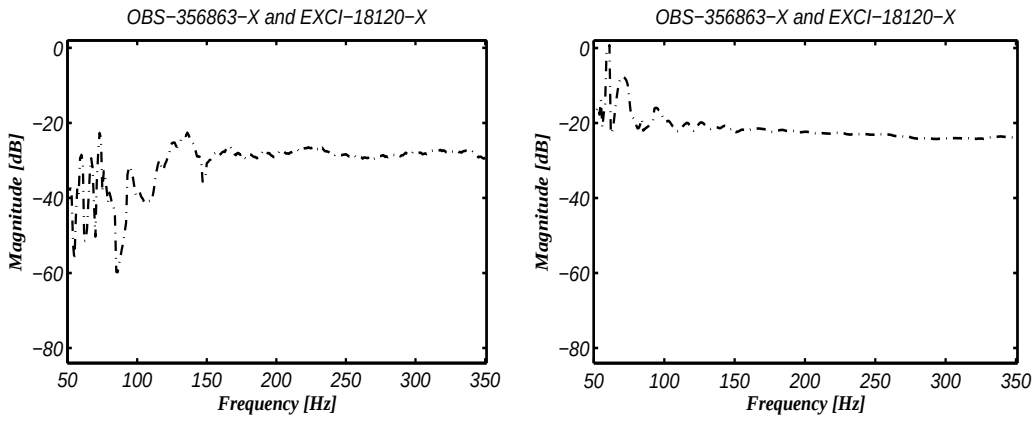

FIG. 4 – $\underline{\mathbf{T}}^{loc}(\omega)$ (Left) and $\mathcal{E}^{loc}(\omega)$ (Right) for a structure excitation and a structure observation points .

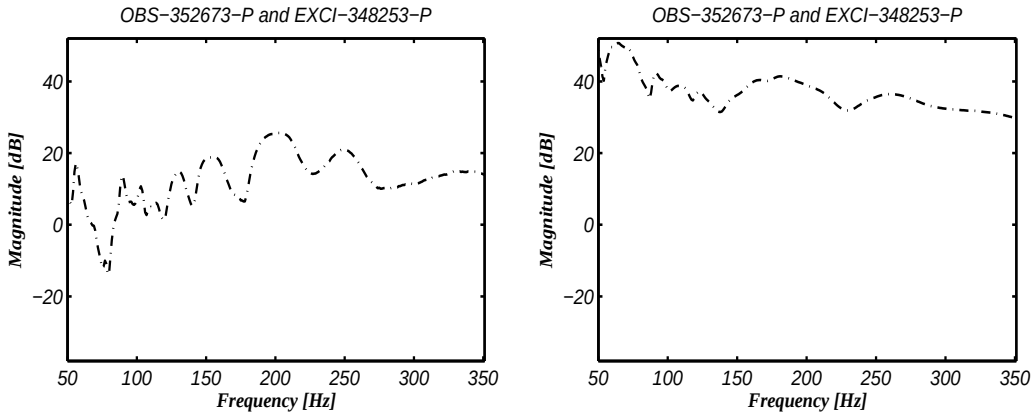

FIG. 5 – $\underline{\mathbf{T}}^{loc}(\omega)$ (Left) and $\mathcal{E}^{loc}(\omega)$ (Right) for a fluid excitation and a fluid observation points.

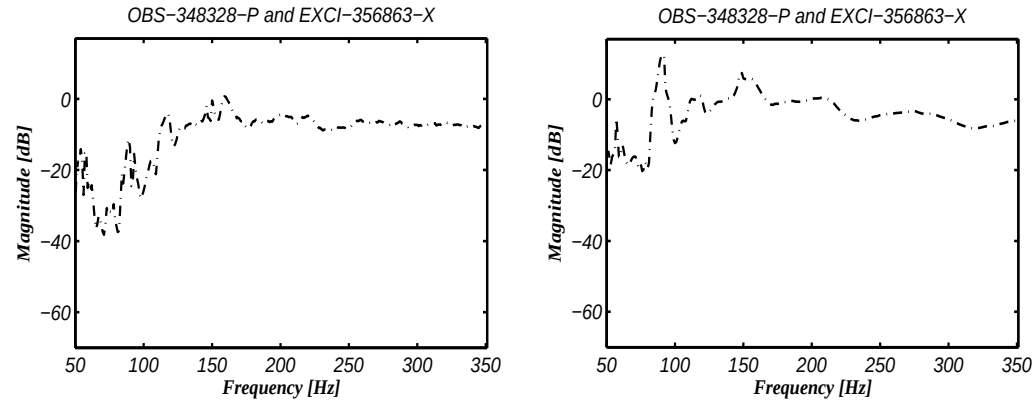

FIG. 6 – $\underline{\mathbf{T}}^{loc}(\omega)$ (Left) and $\mathcal{E}^{loc}(\omega)$ (Right) for a structure excitation and a fluid observation points.

After obtaining $\mathbf{T}^{loc}(\omega,\theta)$ for each realization θ, the local directions of maximum mobility are then calculated using $\underline{\mathbf{T}}(\omega)$. Each realization $\mathbf{T}^{loc}(\omega,\theta)$ is then projected on these directions as explained in Section 5. The input and output mobilities of the vibroacoustic system are calculated for each realization using Eq. (13) and then the value of $\mathcal{E}^{loc}(\omega,\theta)$ is obtained using Eq. (28). The confidence regions of $\mathbf{T}^{loc}(\omega)$ and $\mathcal{E}^{loc}(\omega)$ are constructed using the quantiles [20] with a probability of 0.95. Figs. (4), (5), and (6) show the mean values for $\mathbf{T}^{loc}(\omega)$ and $\mathcal{E}^{loc}(\omega)$ for different types of excitation and of observation points. From the figures, one can notice that the variation in magnitude, as a function of frequency, of $\underline{\mathbf{T}}^{loc}(\omega)$ is less than that of $\underline{\mathcal{E}}^{loc}(\omega)$ especially for the case of structure excitation and structure observation. Moreover, it can be seen that when fixing an observation point and changing the direction of excitation among the three local principal directions or vice versa, $\underline{\mathcal{E}}^{loc}(\omega)$ seem to undergo less changes than $\underline{\mathbf{T}}^{loc}(\omega)$. This is illustrated in Figs. (7) to (9) showing the confidence regions corresponding to a structure observation DOF and three different structure excitation DOF corresponding to the three local principal directions.

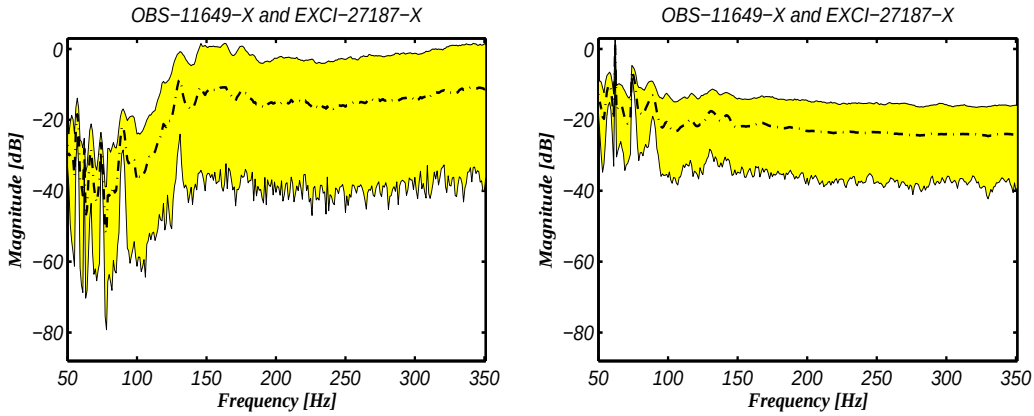

FIG. 7 – Confidence regions of $\mathbf{T}^{loc}(\omega)$ (Left) and $\underline{\mathcal{E}}^{loc}(\omega)$ (Right) observation DOF : Structure-X excitation DOF : Structure-X

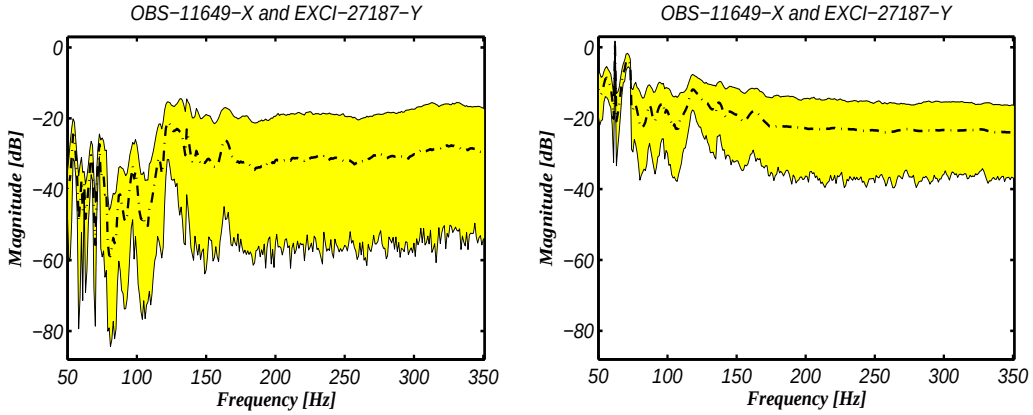

FIG. 8 – Confidence regions of $\mathbf{T}^{loc}(\omega)$ (Left) and $\underline{\mathcal{E}}^{loc}(\omega)$ (Right) observation DOF : Structure-X, excitation DOF : Structure-Y

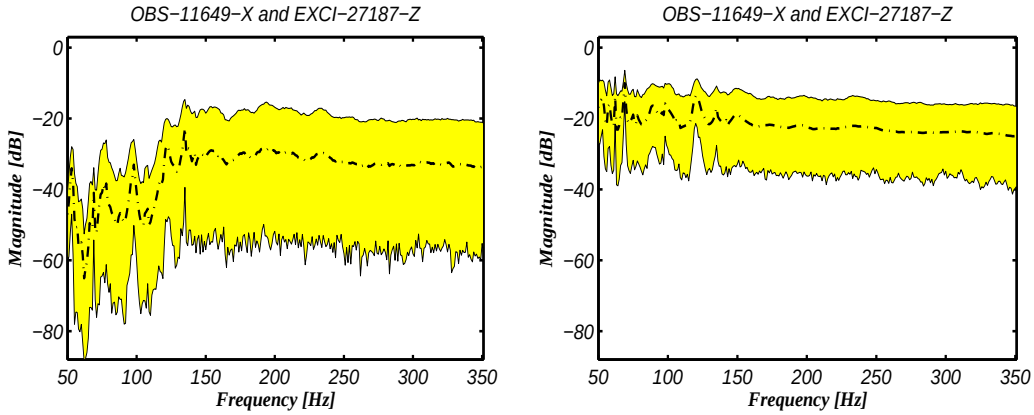

FIG. 9 – Confidence regions of $\mathbf{T}^{loc}(\omega)$ (Left) and $\underline{\mathcal{E}}^{loc}(\omega)$ (Right) observation DOF : Structure-X excitation DOF : Structure-Z

The mean input power as well as the matrix-valued spectral density function of the excitation forces are calculated using $\underline{\mathbf{T}}^{loc}(\omega)$ from which the mean vector-valued spectral density function of the output velocity is obtained. The real number e_{OJ} is evaluated using Eq. (38). The matrix $\epsilon^2_{\mathcal{E}}$ of the errors between $\mathbb{E}_{OJ}(\omega)$ and $\underline{\mathcal{E}}_{loc}(\omega)$ is evaluated using Eq. (40) and the results are plotted for each frequency. Fig. (10) shows the color plots of the $(n_\mu \times n_\nu)$ matrix $\epsilon^2_{\mathcal{E}}$ at 70Hz, 170Hz, 270Hz, and 350Hz.

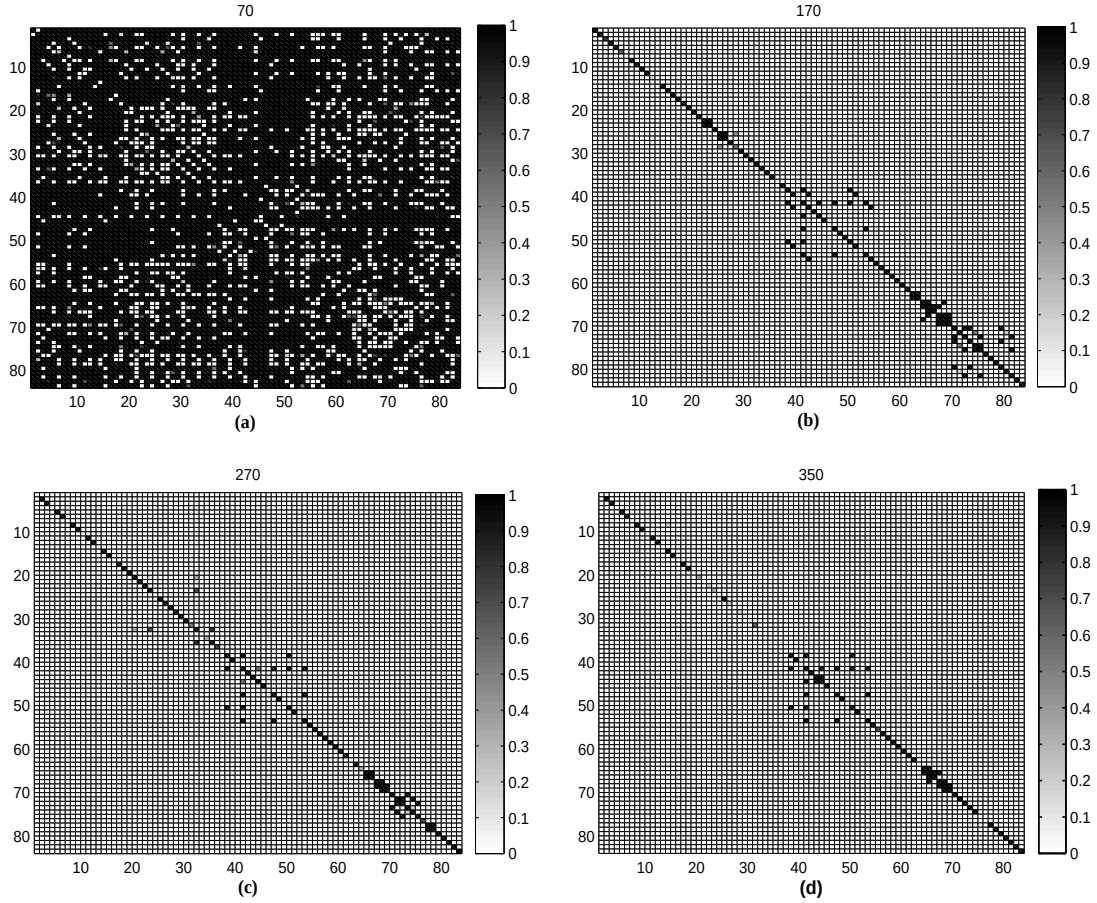

FIG. 10 – color plots of $\epsilon^2_{\mathcal{E}}$ at (a) 70Hz (b) 170Hz (c) 270Hz (d) 350Hz.

From Fig. (10) it can be observed that at low frequency the error between $\mathbb{E}_{OJ}(\omega)$ and $\underline{\mathcal{E}}_{loc}(\omega)$ is high at nearly all elements. At higher frequencies the error decreases away from the block diagonal elements, that means when the hypothesis that the excitation and observation points are far enough from each others is fulfilled. This hypothesis holds true starting at about 170Hz. In what comes This frequency will be called the lower bound frequency. each block on the diagonal of the matrix corresponds to DOF situated on the same part of the structure.

8 Conclusion

An energy based method for vibroacoustic analysis in low- and medium frequency ranges was established. This method is based on the implementation of the non-parametric probabilistic approach in the vibroacoustic modeling process. Using an energy method along with the stochastic model, a simplified vibroacoustic model was elaborated. This model is more robust regarding modeling and parameter uncertainties and also from the

conception point of view. The energy method as well as the simplified model, and the associated hypothesis were verified numerically on an automotive structure and its internal cavity.

Références

[1] C. Soize, *Maximum entropy approach for modeling random uncertainties in transient elastodynamics*, Journal of Acoustical Society of America, Vol. 109, No. 5, (2001), pp. 1979-1996.

[2] C. Soize, *A comprehensive overview of a non-parametric probabilistic approach of model uncertainties for predictive models in structural dynamics*, Journal of Sound and Vibration, Vol. 288, No. 1, (2005), pp. 623-652.

[3] C. Soize, *Random matrix theory for modeling uncertainties in computational mechanics*, Journal of Sound and Vibration, Vol. 194, No. 1, 1333-1366, (2004), pp. 1333-1366.

[4] R.H. Lyon, *Statistical Energy Analysis of Dynamical Systems*, MIT Press (1975), San Diego.

[5] R.H. Lyon, *Statistical Theory and application of statistical energy analysis*, 2nd edition, Butterworth-Heinemann (1995), Boston, MA.

[6] F.J. Fahy, A.D. Mohammed, *A study of uncertainty in applications of SEA to coupled beam and plate systems, partI : Computational experiments*, Journal of Sound and Vibration, Vol. 158, No. 1, (1992), pp. 45-67.

[7] R.S. Langley, P.Bremner, *A hybrid method for the vibration analysis of complex structural-acoustic systems*, Acoustical Society of Smerica , Vol. 105, No. 3, (1999), pp. 1657-1671.

[8] L. Maxit, J.-L. Guyader, *Extention of SEA model to subsystems with non-uniform modal energy distribution*, Journal of Sound and Vibration, Vol. 265, No. 1,(2003), pp. 337-358.

[9] R.S. Langley, A.W.M. Brown, *The ensemble statistics of the band-avaraged energy of random system*, Journal of Sound and Vibration, Vol. 275, No. 1, (2004), pp. 847-857.

[10] R.S. Langley, V. Cotoni, *Response variance prediction in the statistical energy analysis of built up systems*, Acoustical Society Of America, Vol. 115, No. 2, (2004), pp. 706-718.

[11] P.J. Shorter, R.S. Langley, *Vibroacoustic analysis of complex systems*, Journal of Sound and Vibration, Vol. 288, No. 1, (2005), pp. 669-699.

[12] V. Cotoni, R.S. Langley, M.R.F. Kinder, *Numerical and experimental validation of variance prediction in the statistical energy analysis of built-up systems*, MJournal of Sound and Vibration, Vol. 288, No. 1, (2005), pp. 701-728.

[13] N. Totaro, J.L. Guyader, *SEA substructuring using cluster analysis : The MIR index*, Journal of Sound and Vibration, Vol. 290, No. 1, (2006), pp. 264-289.

[14] G. Orefice, C. Caccilati, J.L. Guyader, *The energy mobility*, Journal of Sound and Vibration, Vol. 290, No. 1, (2006), pp. 264-289.

[15] R. Ohayon, C. Soize, *Structural Acoustics and Vibrations*, Academic Press(1998), San Diego.

[16] J.F. Durand, C. Soize, L. Gagliardini, *Structural-acoustic modeling of automotive vehicles in presence of uncertainties and experimental identification and validation*, Journal of Acoustical Society of America, 2008.

[17] J.F. Durand, *Modélisation de véhicules automobiles en vibroacoustique numérique avec incertitudes de modélisation et validation expérimentale*, Phd Theses, Université de Marne-la-Vallée, France(2007).

[18] L. Gagliardini, L. Houillon, G. Borello, L. Petrinelli, *Virtual SEA- FEA based modeling of mid-frequency structure-borne noise*, Journal of Sound and Vibration, Vol. 39, No. 1, Academic Press (2005), pp. 22-28.

[19] Y.K. Koh, R.G. White, *Analysis and control of the vibrational power transmission to machinery supporting structures subjected to a multi-excitation system, partI : Driving point mobility matrix of beams and rectangular plates*, Journal of Sound and Vibration, Vol. 196, No. 4, Academic Press (2007), pp. 469-493.

[20] R.J. Serfling, *Approximation Theorems of Mathematical Statistics*, John Wiley & Sons (1980), New york.